NIST Special Publication
NIST SP 500-340

# Guidance on Contactless Friction Ridge Image Compression, v1.0

John Libert
Shahram Orandi
Kenneth Ko
Bruce Bandini
John Grantham
Craig Watson

This publication is available free of charge from:
https://doi.org/10.6028/NIST.SP.500-340

NIST NATIONAL INSTITUTE OF STANDARDS AND TECHNOLOGY
U.S. DEPARTMENT OF COMMERCE

**NIST Special Publication**
**NIST SP 500-340**

# Guidance on Contactless Friction Ridge Image Compression, v1.0

John Libert
Shahram Orandi
Kenneth Ko
Bruce Bandini
Craig Watson
*Image Group*
*Information Access Division*
*Information Technology Laboratory*

John Grantham
*Systems Plus, Inc.*

This publication is available free of charge from:
https://doi.org/10.6028/NIST.SP.500-340

May 2023


U.S. Department of Commerce
*Gina M. Raimondo, Secretary*

National Institute of Standards and Technology
*Laurie E. Locascio, NIST Director and Under Secretary of Commerce for Standards and Technology*

NIST SP 500-340
May 2023





**Publication History**
Approved by the NIST Editorial Review Board on 2023-04-12

**How to Cite this NIST Technical Series Publication**
Libert J, Orandi S, Ko K, Bandini B, Grantham J, Watson C (2023) Guidance on Contactless Friction Ridge Image Compression. (National Institute of Standards and Technology, Gaithersburg, MD), NIST Special Publication (SP) NIST SP 500-340. https://doi.org/10.6028/NIST.SP.500-340

**NIST Author ORCID iDs**
John Libert: 0000-0003-0796-6871
Shahram Orandi: 0000-0002-5390-6119
Kenneth Ko: 0000-0002-2363-8491
Bruce Bandini: 0000-0003-0608-6426
John Grantham: 0000-0003-2219-0944
Craig Watson: 0000-0001-6045-5806

**Contact Information**
fastcap@nist.gov

## Abstract

Nascent technologies show promise in collecting 500 ppi fingerprints in a contactless fashion while yielding various improvements in the collection process over legacy contact collection methods currently in use throughout the world. While it has been shown that these new devices show promise in producing imagery that may be interoperable with legacy contact collected images [26][33], the contactless devices may be prone to capturing superfluous data (e.g., fingernail, finger background, or other imaging artifacts) pushing existing friction ridge algorithms meant for contact collection beyond those images for which they were originally designed. Image compression algorithms are highly sensitive to information content and complexity of the image being processed [34]. Currently there are two compression algorithms specified for contact-collected fingerprints: WSQ for 500 ppi and JPEG 2000 for the more information-rich 1000 ppi fingerprint imagery [28].

It was hypothesized that the more information-rich contactless-collected imagery, while being captured at the same sample rate as legacy 500 ppi contact-collected fingerprint imagery, may be better suited for the JPEG 2000 specification.

Analysis of automated comparison scores as well as signal quality metrics showed that there was no significant difference found between the two algorithms when processing contactless imagery. Further examination of signal level metrics showed that WSQ remains better able to preserve spectral power of the image in regions of the frequency spectrum typically associated with Level 2 and Level 3 fingerprint features and therefore WSQ appears to be better suited for 500 ppi contactless fingerprint imagery.

## Keywords

500 ppi fingerprint imagery; contactless fingerprint; fingerprint compression; JPEG 2000; PSNR; SIVV; SSIM; Wavelet Scalar Quantization; WSQ.

## Table of Contents



## List of Tables

## List of Figures

## Acknowledgments

We would like to acknowledge and thank the Federal Bureau of Investigation's (FBI) Criminal Justice Information Services (CJIS) Division – Programs Research and Standards Unit (PRSU) who provided funding and support to National Institute of Standards and Technology (NIST) in the development of this Guidance on Contactless Friction Ridge Image Compression.

We also wish to thank Gregory P. Fiumara and John M. Splain for their time, advice, and candor in reviewing the contents of this special publication and providing many meaningful suggestions to help make this a better report.

## Executive Summary

Nascent technologies show promise in collecting 500 ppi[1] fingerprints in a contactless fashion while yielding various improvements in the collection process over legacy contact collection methods currently in use throughout the world.

Observations in previous studies [26][33] showed that while these nascent contactless capture devices can produce imagery that is interoperable with legacy contact collected images, the contactless devices may be prone to capturing superfluous data (e.g., fingernail, finger background, or other imaging artifacts).

This superfluous data in contactless collected fingerprint imagery may have unintended impact on algorithms that comprise the operational processing path of existing contact-collected fingerprint imagery. One such algorithm in the processing path of these images is used for image compression. Compression algorithms can be highly sensitive to information content and complexity of the image being processed [34].

Currently, the specifications for compression of 500 ppi contact-collected images indicates the use of the lossy Wavelet Scalar Quantization (WSQ) algorithm at the compression rate of 0.75 bits per pixel (bpp) [28]. The WSQ algorithm has been designed and optimized for 500 ppi contact-collected fingerprint imagery.

NIST examined challenges with legacy contact-collected 1000 ppi fingerprint imagery which inherently have a higher information content than 500 ppi fingerprint imagery [35][36][37]. In those studies, we examined and established the usage of the general-purpose JPEG 2000 algorithm as an alternative to WSQ to better accommodate the additional information content of 1000 ppi[2] imagery.

For this study, it was hypothesized that newer contactless-collected imagery with additional information content, while being captured at the same sampling rate as legacy 500 ppi contact-collected fingerprint imagery, may not be suitable for WSQ. Instead, a better strategy for contactless compression may be to utilize the compression specifications established for the more information rich 1000 ppi fingerprint imagery instead.

The primary measurand for this analysis is a set of automated matching scores generated by a state-of-the-art law enforcement fingerprint matcher. (Section 3). While the resulting match score can be the ultimate gauge of utility for biometric samples in an automated system, sometimes subtle changes in a biometric sample do not yield a measurable change in the matching score. Because of this, we also processed the treatment images using various signal analysis algorithms that can identify more subtle shifts in image fidelity (Section 4).

For this study, the experimental treatments included the WSQ and JPEG 2000 algorithms to identify the optimal strategy. In all cases, the methodology compared lossy compressed images to images that have never been subjected to lossy compression. Fingerprint imagery from two

[1] 500 ppi = 19.7 pixels per millimeter (ppmm).
[2] 1000 ppi = 9.85 pixels per millimeter (ppmm).

contact and six contactless devices were tested, score distributions for nine compression treatments were examined using the Kruskal-Wallis non-parametric Analysis of Variance.

For each of the eight devices examined, statistical tests found no significant difference in median automated matcher comparison scores among the various compression treatments.

Next, the signal analysis measures showed a slightly higher fidelity with JPEG 2000 over WSQ compression, but closer examination of where the advantages lie in the spectral differences of the images on a frequency band-by-band basis shows that WSQ is better able to preserve spectral power of the image in regions of the spectrum typically associated with Level 2 and Level 3 fingerprint features [38][39].

Given these results, we conclude that while there were no statistically significant differences between matcher score distributions for images compressed using the WSQ and JPEG 2000 specifications, WSQ continues to be a better choice for contactless fingerprint imagery at 500 ppi due to its ability to more effectively preserve Level 2 and Level 3 fingerprint details, thereby rejecting our hypothesis of a possible benefit from utilizing the compression specifications for JPEG 2000 meant for use at 1000 ppi. Moreover, without a compelling reason to change, end users need not alter current practice of using WSQ for compression of 500 ppi friction ridge imagery.

# 1. Introduction

The criminal justice communities throughout the world exchange fingerprint imagery primarily in 8-bit grayscale at a resolution of 500 pixels per inch (ppi)[3]. The Wavelet Scalar Quantization (WSQ) [1]-[7] fingerprint image compression algorithm is currently the recommended algorithm for the compression of 500 ppi fingerprint imagery as specified in the American National Standards Institute/National Institute of Standards and Technology Information Technology Laboratory (ANSI/NIST-ITL) Standard [28].

Since the WSQ specification was designed specifically for 500 ppi contact-collected fingerprint imagery, it was neither validated nor prescribed for use at resolutions other than 500 ppi nor with other capture methodologies such as contactless. JPEG 2000 was selected as the alternative to WSQ for 1000 ppi fingerprints as well as other friction ridge biometrics captured at 1000 ppi such as palms. The JPEG 2000 CODEC can operate effectively across a variety of source image formats, resolutions, and color depths. Hence, while not designed or tuned specifically for the compression of fingerprints, the modern JPEG 2000 [8][9][12][13]standard provides flexibility to allow for its utilization in the compression of friction ridge imagery. It should be noted that, like WSQ, JPEG 2000 is a wavelet-based image transformation algorithm, but unlike WSQ, JPEG 2000 implementations are more widely available in general purpose commercial off-the-shelf (COTS) products as well as no-cost open-source implementations.

Both WSQ and JPEG 2000 are "lossy"[4] compression algorithms. Lossy compression algorithms employ data encoding methods that discard (lose) some of the data in the encoding process to achieve a larger reduction in the storage space required by the data after being compressed. The discarded information is considered an acceptable level of loss if it does not hinder the use of the compressed image or, in some cases, determined to lie beyond the perceptual capacity of the observer. Decompressing (decoding) the resulting compressed data yields output that, while different from the original, is ideally similar enough to the original that it remains useful for the intended purpose. *Lossless* compression algorithms on the other hand can produce a compressed image that can be decompressed back to original form with no loss or change to the resulting image. The disadvantage to lossless compression algorithms is that they produce compressed images that can be many times larger in file size than those produced by lossy algorithms.

NIST has issued several guidance recommendations for use of JPEG 2000 to compress 1000 ppi[5] friction ridge images. NIST Special Publication 500-289 [14] specifies application of the JPEG 2000 CODEC to 1000 ppi fingerprint images. This specification was extended to 1000 ppi palm and whole hand impressions in [17]. Now we have the emergence of technology to capture fingerprint images without the device contacting the friction ridge skin– termed "contactless fingerprint acquisition." Because of differences between fingerprint images captured by contactless devices versus those acquired through contact, the question has been raised as to which CODEC, if any, would be most appropriate for compression of contactless fingerprint images. Inasmuch as contactless fingerprints are currently acquired at a target sample rate of 500

[3] 500 ppi = 19.7 pixels per millimeter (ppmm).

[4] JPEG 2000 has a lossless mode able to achieve a compression ratio of approximately 1.5:1, but the main interest in this CODEC for biometric samples involves only the lossy mode.

[5] 1000 ppi = 39.4 pixels per millimeter (ppmm)

ppi, then encoding imagery with WSQ [5] should be acceptable. Thus, the objective of the present investigation is to evaluate via various fidelity measures which of the two codecs are most appropriate for compression of contactless fingerprints – WSQ at the standard 0.75 bits per pixel (bpp) or JPEG 2000. Because WSQ compression at 0.75 bpp results in compression ratios (CRs) that averages about 15:1 (as will be seen below), JPEG 2000 compression at 15:1 is examined in comparison.

## 2. Method

### 2.1. Image Data

As source images we use contact and contactless images collected from Federal Government volunteers at NIST in May-June 2019 and used for NIST Interagency Report (NISTIR) 8307 [29] and NISTIR 8315 [33][29]. These data[6] consisted of fingerprints acquired from approximately 200 donors using two contact devices, two desktop stationary contactless devices, and four smartphone fingerprint capture applications running on both Android and iOS devices. In the present document, we follow the anonymized device naming as follows:

Table 1 – Fingerprint Devices

| | |
|---|---|
| Dev01 | Frustrated Total Internal Reflection (FTIR) Contact |
| Dev02 | Thin Film Transistor Electro-Luminescent Contact |
| Dev03 | Desktop Stationary Contactless |
| Dev04 | Desktop Stationary Contactless |
| Dev05 | Smartphone Application Contactless |
| Dev06 | Smartphone Application Contactless |
| Dev07 | Smartphone Application Contactless |
| Dev08 | Smartphone Application Contactless |

The control device, Dev01, was used to collect two encounters of slap-four impressions from left and right hands at a sample rate of 500 ppi. The first encounter was singularly used as the exemplar for all comparisons against the seven other devices. The second encounter provided a control comparison to use as a benchmark or "high bar." Dev02 was used to collect a single set of slap-four impressions from left and right hands to provide a contact-to-contact interoperability baseline. This second contact device, Dev02, employed an electro-luminescent technology for image formation.

Contact slap-four impressions were segmented into individual fingerprint images that were labeled following the finger numbering scheme depicted in Figure 1 where finger #2 is the right-hand index finger:

[6] Referred to as the "2019 imagery" in subsequent sections of this document.

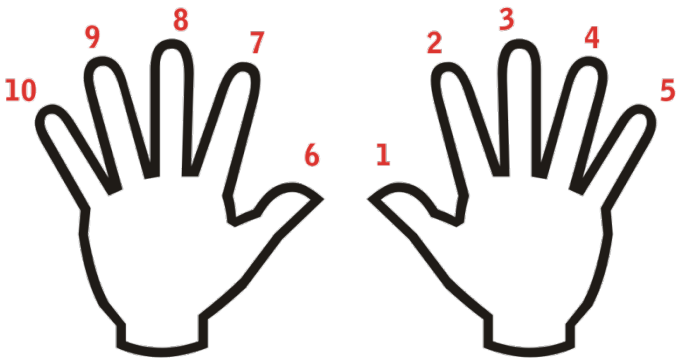


Figure 1 – Finger Numbering Methodology

As a best practice, we limited the time required to collect the images with all the devices by not capturing thumbs. Thus, fingers numbered 1 and 6 were excluded from the collection and from the present analysis.

## 2.2. Image Compression

### 2.2.1. Rate Control in Compression

The first issue we must confront is that comparisons of WSQ and JPEG 2000 can be more challenging given the differences in the rate control mechanism utilized by each respective CODEC. The compression rate of the WSQ CODEC is controlled by setting the *desired* target bit rate. The actual resulting compression ratio will vary to be more forgiving (and less aggressive in compressing) according to the textural complexity of the image. On the other hand, the Open JPEG CODEC [13]used by NIST is provided a target compression ratio and the CODEC will compress images to achieve that compression ratio target regardless of the image texture degradation. If we specify to Open JPEG that its output should be compressed 15:1, the resulting images will be compressed to 15:1 with very little variation from that target value. Figure 2 demonstrates this behavior and displays distributions of measured compression ratios[7] for the 2019 imagery subjected to WSQ compression at 0.75 bpp and JPEG 2000 compression at 15:1. WSQ compression at 0.75 is specified for yielding an approximately 15:1 compression ratio. As seen in Figure 2 the median compression ratio resulting from specifying a target bit rate for WSQ yields actual (median) compression ratios that vary between approximately 12:1 and 18:1. By contrast, we see that for Open JPEG the median compression ratio varies only slightly

[7] Compression ratio generally refers to comparative size on disk. We can use the size of the compressed code stream in bytes but because the source and decoded files are stored on disk using Programable Network Graphics (PNG) format that is already losslessly compressed, we compute uncompressed file size as width x height x 1 byte. Thus, Compression Ratio (CR) = uncompressed file (image) size/compressed file size.

from the designated target value. The median values[8] for all the source devices lie between 15.0 and 15.2. (See Appendix A for a key to box and whisker plots).

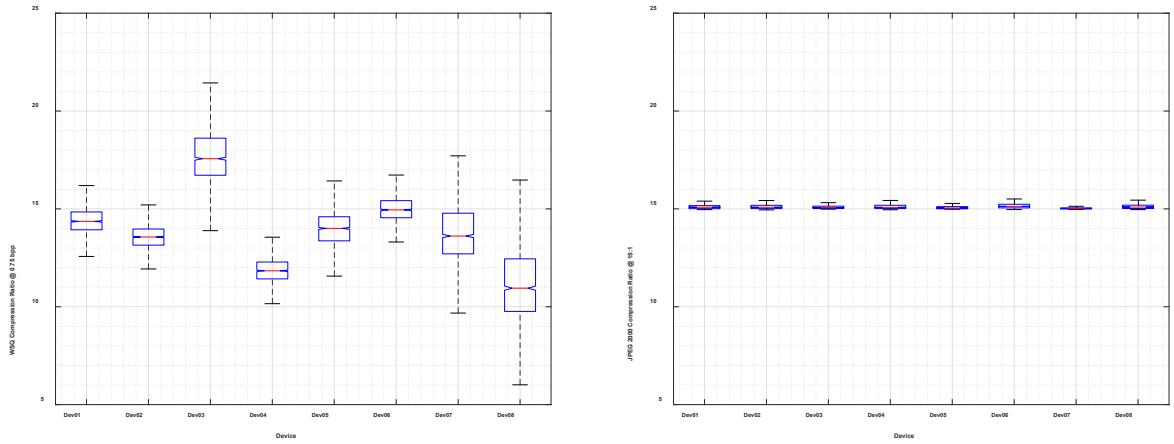


Figure 2 – Calculated compression ratios for 2019 imagery compressed with WSQ at 0.75 bpp (left) and Open JPEG 2000 at 15:1 (right).

### 2.2.2. WSQ

All images were encoded with the NIST WSQ CODEC [10][11]. To correctly utilize images with width and height dimensions less than the minimum acceptable for the WSQ algorithm (defined as 256 pixels by 256 pixels), those images were padded to the minimum size using pixels of value 255 (white). These additional pixels were added to the periphery (all four sides equally) of the captured image to raise it to the required minimum dimension. For analysis, the WSQ code streams were decoded and stored losslessly as Portable Network Graphic (PNG) format files. While several bit rates are supported by the WSQ CODEC, the standard for 500 ppi fingerprint submittals to the Federal Bureau of Investigation (FBI) and other Law Enforcement Organizations (LEOs) is WSQ compression at a bit rate of 0.75 bpp. This translates to a compression ratio of approximately 15:1 on average, as shown in Figure 2.

### 2.2.3. JPEG2000

The Open JPEG [13] implementation of the JPEG 2000 CODEC was applied to all images and each of the code streams was decoded for analysis. For this implementation of the CODEC, we specify the desired CR; the ratio of input file storage size to output file storage size. The CR we have specified for 1000 ppi fingerprints and palm images is 10:1. This rather conservative specification derives from observations in [14] that variation in the area of white space in the friction ridge image, as well as its textural complexity, may result in variable degrees of

[8] All analyses and graphics in the present paper were done using MATLAB [30]

degradation by a CODEC using a compression ratio target for rate control (see Figure 2). The compression ratio of 10:1 was found to retain both Level 2 and Level 3 detail [17][18] regardless of impression type or friction ridge area imaged. However, in the present instance we wish to compare the two CODECs (WSQ and JPEG 2000) at comparable levels of compression. Hence, we applied JPEG 2000 at the compression ratio of 15:1, as this corresponds to the average effective compression ratio for WSQ at 0.75 bpp.

# 3. Impact of Compression on Automated Fingerprint Comparison

The question is posed as to the relative effect of compression methods on machine comparison using a state-of-the art law enforcement grade fingerprint comparison system: Does the choice of CODEC affect the score distributions obtained for contact and contactless fingerprint samples?

Automated comparison via a law enforcement matcher is a useful metric by which to evaluate utility of a biometric. Accordingly, in Section 3, we test for significant differences among aggregate comparison score distributions and apply error analysis via Area Under the ROC Curve (AUC). Later, in Section 4, we apply selected fidelity metrics to compare effects of the two CODECs on non-compressed source images.

## 3.1. Comparison Test Procedure

### 3.1.1. Image Data

The fingerprint images collected in 2019 and examined in [29] and [33] were again used for testing. For simplicity, comparisons were made using eight fingers, i.e., finger positions 2 – 5 for the right hand and 7 – 10 for the left hand. Experiments were set up on NIST's law enforcement matcher.

### 3.1.2. Galleries

Three galleries were constructed: The first was composed of non-compressed mates of the probe images together with a non-mate background of 10 million 10-print records[9]. The exemplar mates are the first of two encounters collected as plain contact impressions using an FTIR optical device (Dev01). The background images are stored in WSQ compressed format at the standard 0.75 bpp.

The second gallery was composed of the same mate images as the first, except that in this case, the images were subjected to one cycle of WSQ compression at 0.75 bpp and then decoded and saved to the PNG image format for input to the matcher. We save decoded images to PNG format to avoid effects of the comparison system's proprietary WSQ decoder.

A third gallery included the contact mates (as described above) compressed with the Open JPEG CODEC at the compression ratio of 15:1. The 10 million background records were as previously described.

[9] These are operationally collected ten-print records contributed to NIST by law enforcement organizations to support biometric testing activities. Fingerprint images of these ANSI/NIST-ITL records are stored as WSQ code files at 0.75 bpp.

### 3.1.3. Probes

The probes consisted of eight fingerprints collected from each of approximately 200 donors with each of eight devices. These probe images were submitted to the matcher in PNG format for three cases: non-compressed, WSQ encoded/decoded at 0.75 bpp, and JPEG 2000 encoded/decoded at 15:1.

### 3.1.4. Comparisons

Comparison experiments were run on the matcher separately for each of the eight devices:

Table 2 – Test Treatments/Compression Conditions

| Treatment | Gallery | Probes |
|---|---|---|
| 1 – NC_NC | Non-compressed mates + background | Non-compressed |
| 2 – NC_WSQ | Non-compressed mates + background | Encoded/Decoded WSQ @ 0.75 bpp |
| 3 – NC_JP2K | Non-compressed mates + background | Encoded/Decoded JPEG 2000 at 15:1 |
| 4 – WSQ_NC | WSQ Compressed mates + background | Non-compressed |
| 5 – WSQ_WSQ | WSQ Compressed mates + background | Encoded/Decoded WSQ @ 0.75 bpp |
| 6 – WSQ_JP2K | WSQ Compressed mates + background | Encoded/Decoded JPEG 2000 at 15:1 |
| 7 – JP2K_NC | JPEG 2000 compressed mates + background | Non-compressed |
| 8 – JP2K_WSQ | JPEG 2000 compressed mates + background | Encoded/Decoded WSQ @ 0.75 bpp |
| 9 – JP2K_JP2K | JPEG 2000 compressed mates + background | Encoded/Decoded JPEG 2000 at 15:1 |

For each probe, the matcher returns a candidate list of similarity scores for up to 220 candidates. For cases in which the actual mate could not be found among the top 220 candidates, the lowest observed score from an unmated search was used for subsequent analysis.

## 3.2. Analysis

### 3.2.1. Test for Statistical Difference in Medians

The Kruskal-Wallis test [32] examines a matrix for significant difference among the medians of the columnar values where each column represents members of a different group or different treatment. In the present case, we examine the compression conditions for each device to determine if the score distribution for any compression treatment differs from the others. This procedure tests the null hypothesis that the compression treatments (columns of the matrix) come from the same distribution. The alternative hypothesis is that not all samples come from the same distribution. We set the probability of incorrectly rejecting the null hypothesis (alpha) at 0.05.

Each of the following figures exhibits the comparison score distributions for the set of compression treatments consisting of compression state of the exemplars (or gallery) and that of the probes. The compression states are designated as

- NC – no compression

- WSQ – WSQ compression at 0.75 bpp followed by decoding to PNG format for input to the NIST law enforcement grade fingerprint comparison system
- JP2K – JPEG 2000 compression at 15:1

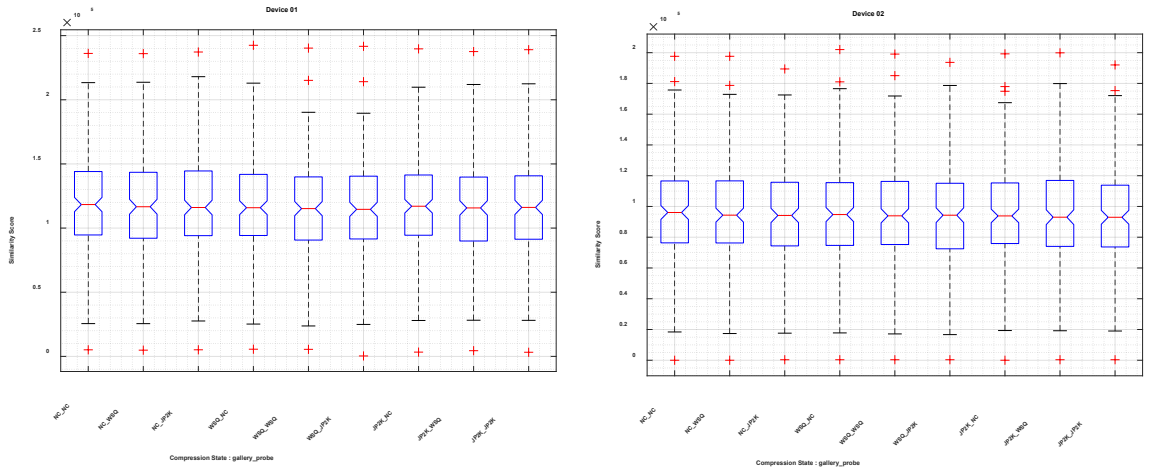


Figure 3 – Distribution of comparison scores for Device 01 (left) and Dev02 (right) under the nine compression states of reference gallery and probe.

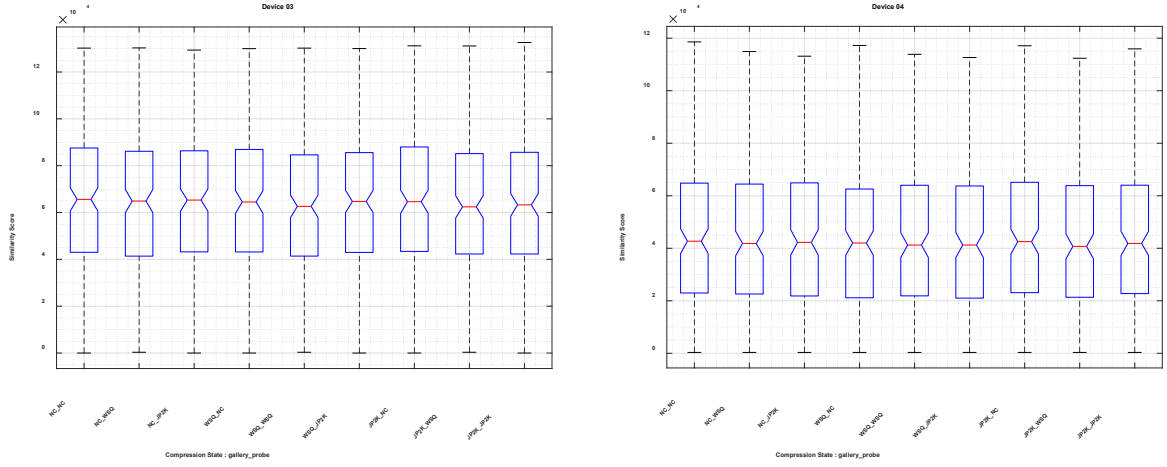


Figure 4 – Distributions of comparison scores for Device 03 (left) and Device 04 (right) under the nine compression states of reference gallery and probe.

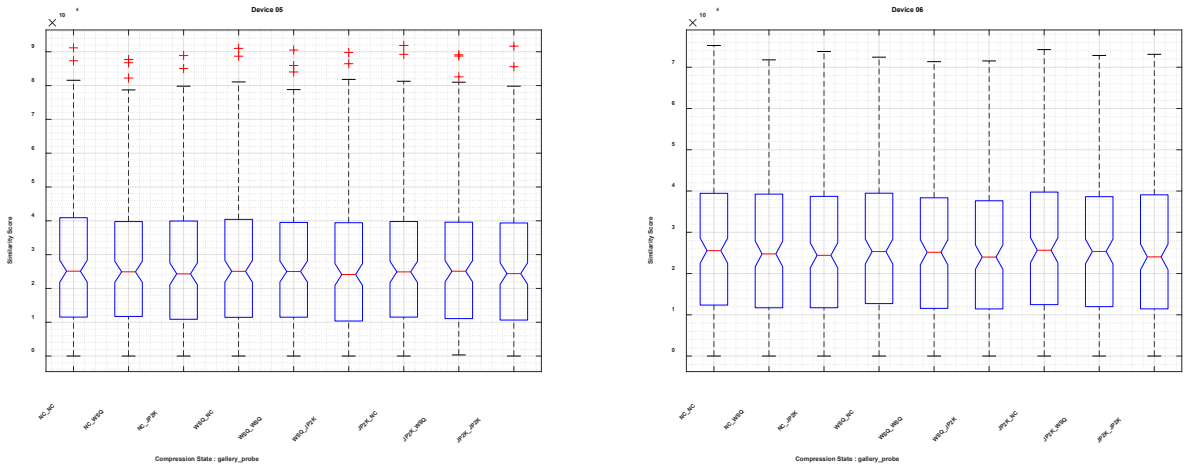


Figure 5 – Distributions of comparison scores for Device 05 (left) and Device 06 (right) under the nine compression states of reference gallery and probe.

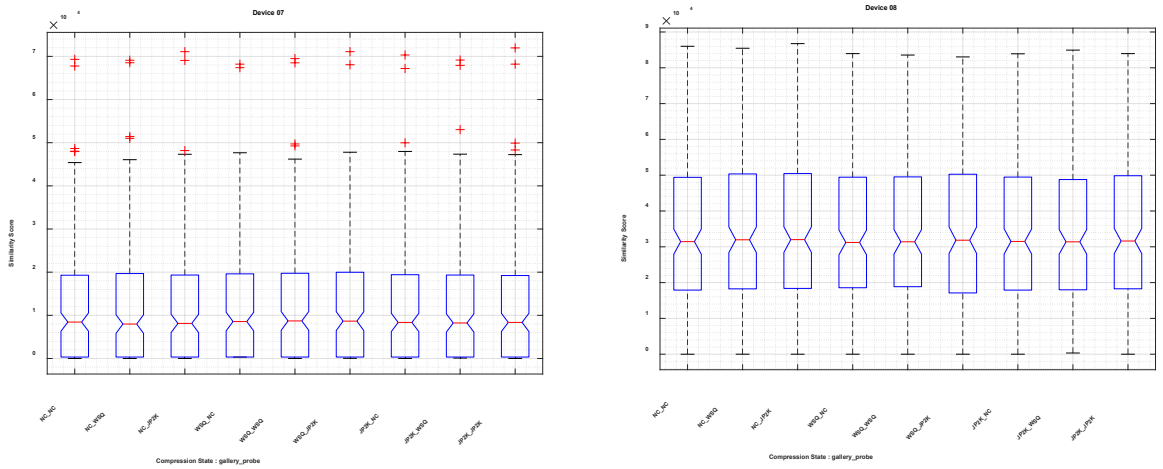


Figure 6 – Distributions of comparison scores for Device 07 (left) and Device 08 (right) under the nine compression states of reference gallery and probe.

We see in Figure 3 - Figure 6 that comparison score distributions remain indistinguishable across all compression treatments of exemplar and probe images. The Kruskal-Wallace Analysis of Variance (ANOVA) summarized in Table 3 finds **p >> 0.05** for each of the eight devices indicating that for each case the sample distributions are drawn from the same population. Hence, we accept the null hypothesis that no significant differences are found among the samples for any of the nine exemplar/probe compression treatments.

Table 3 – Kruskal-Wallace ANOVA

| Device | Source | SS | df | MS | Chi-sq | Prob>Chi-sq |
|---|---|---|---|---|---|---|
| | **Columns** | 624 032.51 | 8.00 | 78 004.06 | 2.45 | **0.964** |
| **D01** | **Error** | 442 934 895.49 | 1 737.00 | 254 999.94 | | |
| | **Total** | 443 558 928.00 | 1 745.00 | | | |
| | **Columns** | 371 984.96 | 8.00 | 46 498.12 | 1.43 | **0.994** |
| **D02** | **Error** | 457 047 152.04 | 1 755.00 | 260 425.73 | | |
| | **Total** | 457 419 137.00 | 1 763.00 | | | |
| | **Columns** | 358 395.59 | 8.00 | 44 799.45 | 1.34 | **0.995** |
| **D03** | **Error** | 478 387 746.91 | 1 782.00 | 268 455.53 | | |
| | **Total** | 478 746 142.50 | 1 790.00 | | | |
| | **Columns** | 164 931.19 | 8.00 | 20 616.40 | 0.62 | **1.000** |
| **D04** | **Error** | 471 135 528.81 | 1 773.00 | 265 727.88 | | |
| | **Total** | 471 300 460.00 | 1 781.00 | | | |
| | **Columns** | 142 588.67 | 8.00 | 17 823.58 | 0.53 | **1.000** |
| **D05** | **Error** | 485 569 576.83 | 1 791.00 | 271 116.46 | | |
| | **Total** | 485 712 165.50 | 1 799.00 | | | |
| | **Columns** | 100 455.59 | 8.00 | 12 556.95 | 0.40 | **1.000** |
| **D06** | **Error** | 440 972 339.91 | 1 737.00 | 253 870.09 | | |
| | **Total** | 441 072 795.50 | 1 745.00 | | | |
| | **Columns** | 136 965.66 | 8.00 | 17 120.71 | 0.54 | **1.000** |
| **D07** | **Error** | 447 687 302.34 | 1 773.00 | 252 502.71 | | |
| | **Total** | 447 824 268.00 | 1 781.00 | | | |
| | **Columns** | 27 685.70 | 8.00 | 3 460.71 | 0.10 | **1.000** |
| **D08** | **Error** | 471 410 167.80 | 1 773.00 | 265 882.78 | | |
| | **Total** | 471 437 853.50 | 1 781.00 | | | |

### 3.2.2. Area Under Curve (AUC) Comparisons[10]

The previous statistical examination of comparison score distributions does not evaluate relative error rates of automated comparison. We would like to resolve False Non-Identification Rate (FNIR), or its inverse, True Positive Identification Rate (TPIR) as well as False Positive Identification Rate (FPIR). Unfortunately, the small sample size (N = 194) for each set of device image captures of our dataset does not permit us to resolve these at a high level of confidence. In particular, the FPIR measurement is limited to $1/194 \approx 5 \times 10^{-3}$ for a single false positive error. Accordingly, we compare the compression conditions using the Area Under the ROC Curve (AUC) [31] for each of the eight devices. Each AUC value is displayed with 95 % confidence interval[11].

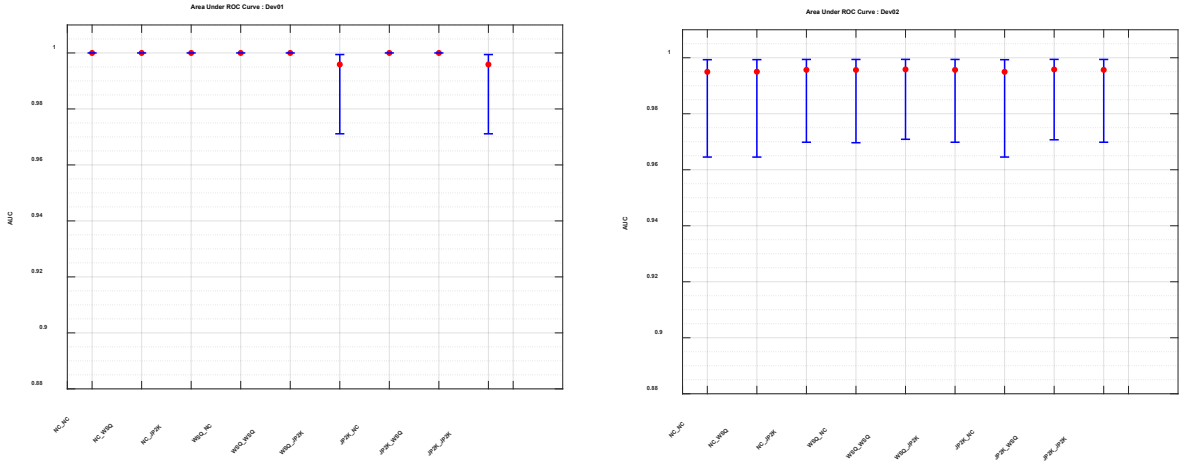


Figure 7 – AUC plots for comparison scores for the nine combinations of image compression applied to exemplar and probe images for Device 01 (left) the control contact device employing FTIR imaging technology and for Device 02, a second contact device using electroluminescent imaging technology.

In Figure 7 we see near-perfect comparison performance with two sets of images collected on the same contact acquisition device. All but two of the lines of the ROC plot are overlain at 1.0. We see slightly lower performance for two treatments involving JPEG 2000 at 15:1, but given the large uncertainty shown in the AUC plot, we might easily consider contact-to-contact comparison with the same device to be unaffected by image compression.

We see consistent performance across all compression treatments for Device 02, a second contact device that captures fingerprints using light-emitting sensor (LES) technology. The slight depression in AUC might be expected as images collected with this contact device are compared to exemplars acquired using a different contact capture technology.

[10] AUC with confidence intervals derived via logistic regression are computed using a MATLAB function by Brian Lau https://github.com/brian-lau/MatlabAUC

[11] Upper confidence bound is truncated to 1.0.

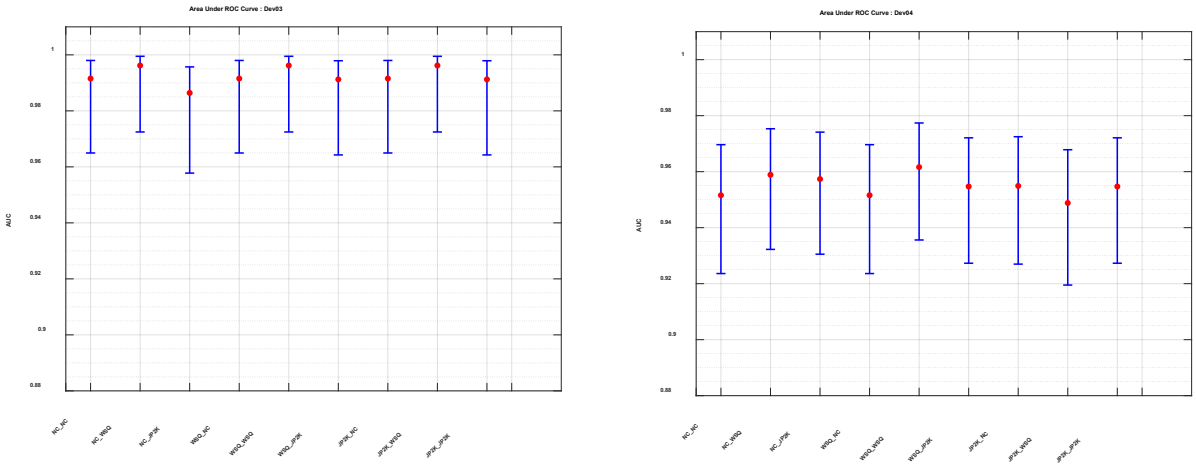


Figure 8 AUC plots for comparison scores for the nine combinations of image compression applied to exemplar and probe images for Device 03 (left) and Device 04(right), both desktop, stationary contactless acquisition devices.

In Figure 8 we see some small variation in AUC among the compression treatments, but all well within the 95 % confidence intervals. We do see slightly lower AUC values for Dev04 compared to Dev03 that performs almost at the level of contact-to-contact comparison.

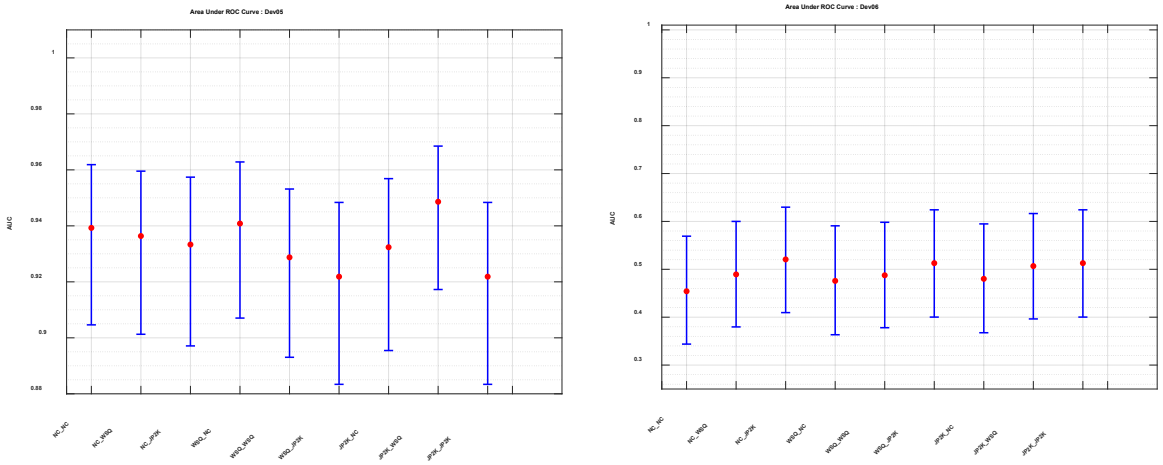


Figure 9 - AUC plots for comparison scores for the nine combinations of image compression applied to exemplar and probe images for Device 05 (left) and Device 06, both smartphone (mobile) contactless acquisition devices.

Figure 9 again shows variation in the AUC among the compression treatments for Devices 05 and 06 but overlap of the 95 % confidence intervals suggests the observed differences are not statistically significant.

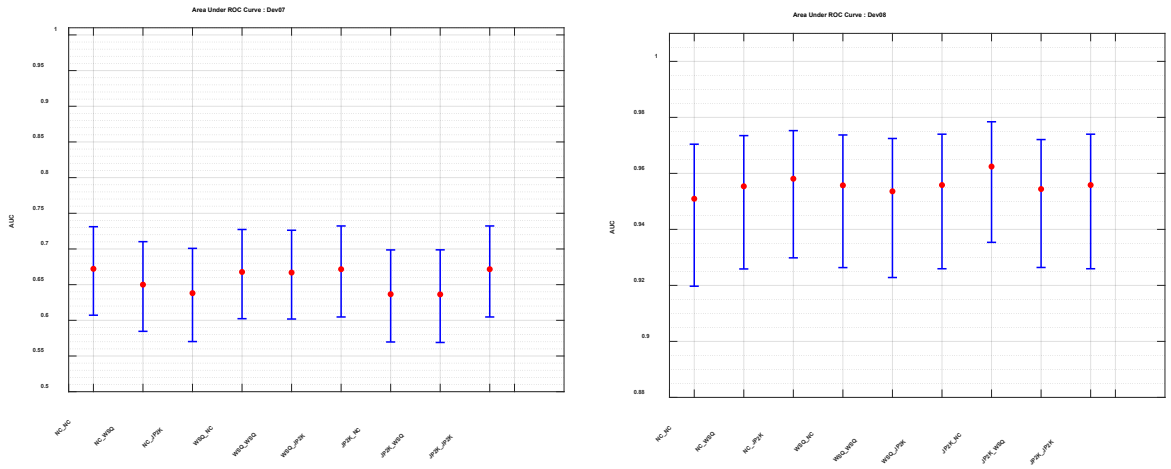


Figure 10 - AUC plots for comparison scores for the nine combinations of image compression applied to exemplar and probe images for Device 07 (left) and Device 08, both smartphone (mobile) contactless acquisition devices.

Similar AUC distributions are seen for Devices 07 and 08 as shown in Figure 10.

## 4. Fidelity Measurement Results

Various fidelity measures are applied to images decoded from the WSQ and JPEG 2000 code streams (compressed image data). The measurements are displayed as box and whisker plots. In each case, distributions for WSQ at 0.75 bpp are displayed in the left of each subfigure, JPEG 2000 at a 15:1 CR on the right subfigure.

### 4.1. Peak Signal to Noise Ratio (PSNR)

First, we compare using Peak Signal to Noise Ratio (PSNR) . PSNR can be used as a fidelity metric in comparing versions of a source image having been subjected to different processes. Typically, we compare the processed image to its unprocessed source image. In this context, a higher PSNR value indicates greater similarity between the source and processed images. Thus, given two images, *f* and *g*, both of dimension *m x n* we can evaluate the overall change in pixel values (in decibels) as

$$PSNR = 20\log_{10}\left(\frac{MAX_f}{\sqrt{MSE}}\right)$$

$$where\ the\ MSE\ (Mean\ Squared\ Error)\ is: \qquad (1)$$

$$MSE = \frac{1}{mn}\sum_{1}^{m}\sum_{1}^{n}\left\|f(i,j) - g(i,j)\right\|^2$$

In eq. (1) *i* and *j* are indices to image pixels.

Referring to Figure 11, we see considerable variation in PSNR with both CODECs across the various devices. In most cases, we see small improvements in PSNR with JPEG 2000 at a 15:1 CR over WSQ CODEC at 0.75 bpp. Devs 04 and 08 are exceptions.

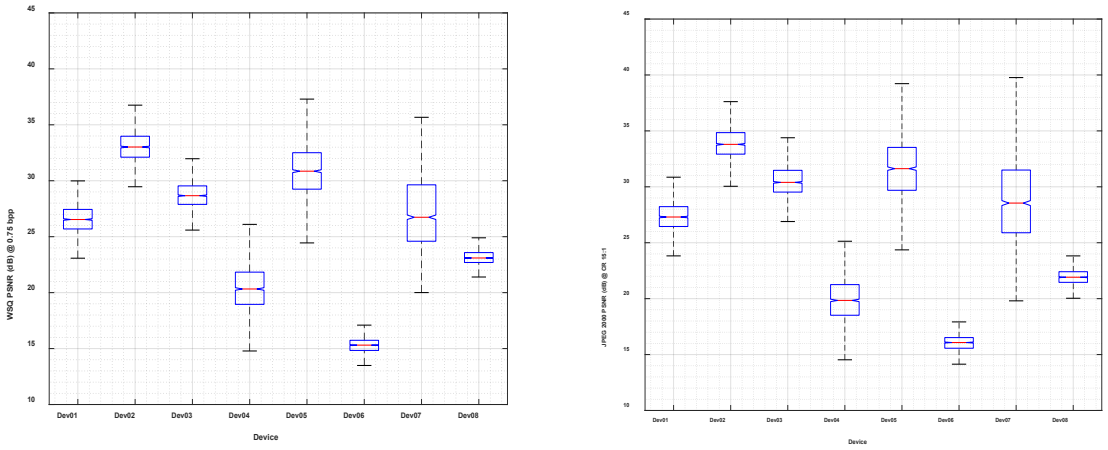


Figure 11 – PSNR for images compressed with a WSQ CODEC at a bit rate of 0.75 bpp (left) and images compressed with a JPEG 2000 CODEC at a target compression ratio of 15:1 (right).

## 4.2. Structural Similarity Index Metric (SSIM)

PSNR is sometimes criticized as being particularly susceptible to spurious degradation due to small global changes in pixel values that are unrelated to the local structure in the image [19][20][21][21]. The Structural Similarity Index Metric (SSIM) [23][24][25][26] overcomes this limitation of PSNR as a fidelity measure. The SSIM is based on the multiplicative combination of three terms, namely the luminance term, the contrast term, and the structural term.

$$SSIM(x,y) = \left[l(x,y)\right]\alpha \bullet \left[c(x,y)\right]\beta \bullet \left[s(x,y)\right]\gamma$$

*where*

$$l(x,y) = \frac{2\mu_x\mu_y + C_1}{\mu_x^2 + \mu_y^2 + C_1},$$

$$c(x,y) = \frac{2\sigma_x\sigma_y + C_2}{\sigma_x^2 + \sigma_y^2 + C_2},$$

$$s(x,y) = \frac{\sigma_{xy} + C_3}{\sigma_x\sigma_y + C_3}, \qquad (2)$$

Where $\mu_x, \mu_y, \sigma_x, \sigma_y,$ and $\sigma_{xy}$ are local means, standard deviations, and cross-covariance for images *x, y*.

By default, regularization constants for the three components, luminance, contrast, and structure are

- *C1 = (0.01*L)^2*, where *L* is the specified dynamic range value of 255.
- *C2 = (0.03*L)^2*, where *L* is the specified dynamic range value of 255.
- *C3 = C2/2.*

The SSIM function uses these regularization constants to avoid instability for image regions where the local mean or standard deviation is close to zero. Therefore, small non-zero values are calculated and used for these constants.

We set $\alpha = \beta = \gamma = 1.0$. This simplifies the formula to

$$SSIM(x,y) = \frac{(2\mu_x\mu_y + C_1)(2\sigma_{xy} + C_s)}{(\mu_x^2 + \mu_y^2 + C_1)(\sigma_x^2 + \sigma_y^2 + C_3)} \qquad (3)$$

The SSIM values of equation (3), evaluated in 8x8 pixel moving image blocks, yield an array of SSIM values. These are pooled by averaging to yield for the image comparison a single figure of merit, the Mean SSIM, sometimes labeled the MSSIM.

Figure 12 shows SSIM distributions for WSQ at 0.75 bpp and JPEG 2000 at 15:1. JPEG 2000 exhibits increases in SSIM for the images captured by all devices with 15:1. This suggests that JPEG 2000 at 15:1 preserves the structural information of the fingerprint images slightly better than WSQ but with comparable variation.

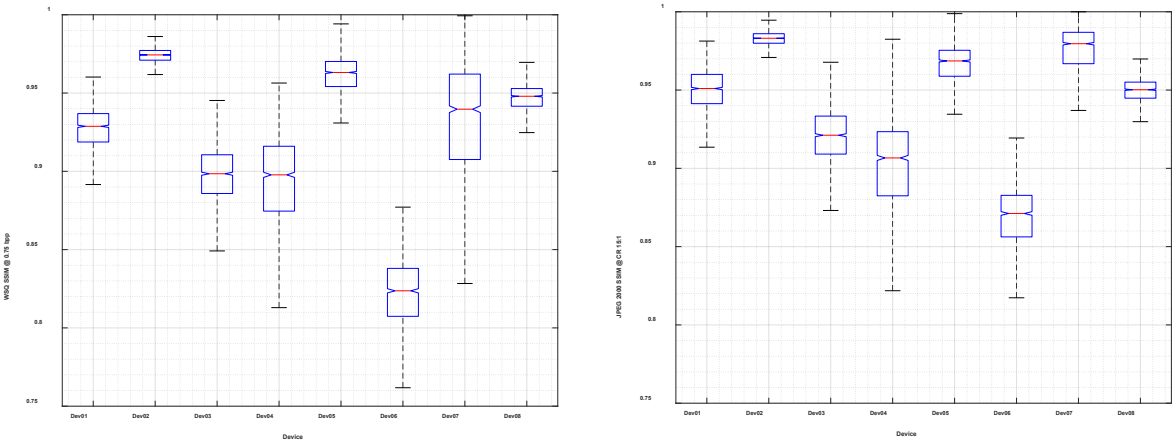


Figure 12 – SSIM for images compressed using a WSQ CODEC at 0.75 bpp (left) and images compressed with a JPEG 2000 CODEC at a target compression ratio of 15:1 (right).

## 4.3. Inverse RMS Difference of Spectral Image Validation Verification (SIVV) Signals

Either differences or ratios of SIVV [16] signals can provide quantitative measures for the comparison of images. For the present study, we examine image differences between pairs of images, $I'_A$ and $I'_B$, with respect to the Root Mean Squared Difference (RMSD) between their two SIVV signals, $\mathbf{s}_1$ and $\mathbf{s}_2$, over the entire frequency range 0 - 0.5 cycles/pixel. Small values of this metric are better but to display values of this metric (as with other measures used in this study) such that a higher score is better, we subtract the SIVV RMSD from 1.0.

$$1.0 - RMSD(\mathbf{s}_1, \mathbf{s}_2) = \sqrt{\frac{\sum_{i=1}^{n} (\mathbf{s}_{1,i} - \mathbf{s}_{2,i})^2}{n}} \qquad (4)$$

where $n = \mathbf{s}_1 = \mathbf{s}_2$ (i.e., the lengths of the signal vectors).

Examination of Figure 13 shows that as with the SSIM, we have in the Inverse SIVV RMSD another structural metric that indicates better median fidelity with JPEG 2000 at 15:1 with reduced variability as well.

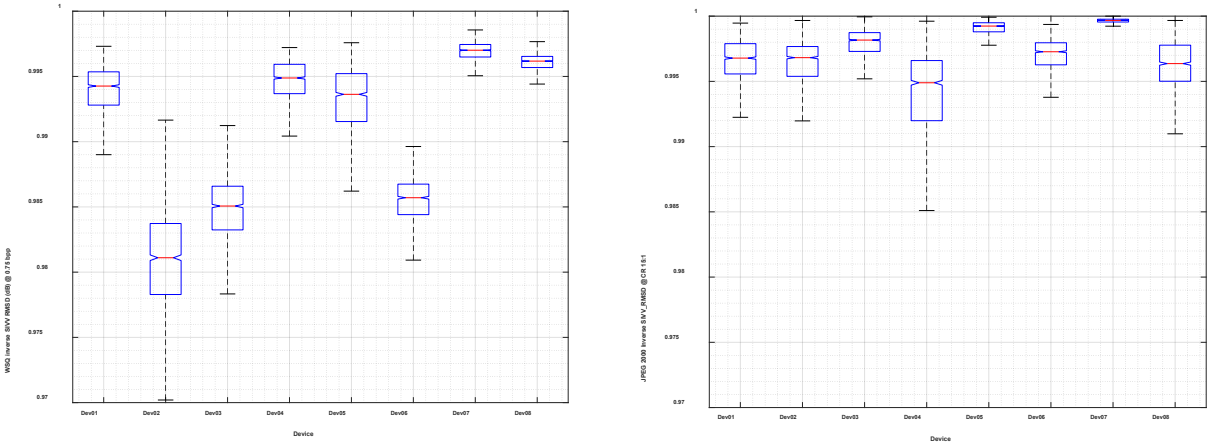


Figure 13 – Inverse SIVV RMSD for images compressed with a WSQ CODEC at 0.75 bpp (left) and images compressed with a JPEG 2000 CODEC at a target compression ratio of 15:1 (right).

## 4.4. Correlation of SIVV Signals

The RMSD measures the total deviation of point-wise comparison of the SIVV signals. The Pearson product moment correlation coefficient measures the parallelism between the two signals irrespective of the magnitude of the difference between them. Accordingly, we compute the correlation coefficient between $\mathbf{s}_1$ and $\mathbf{s}_2$ as

$$r(\mathbf{s}_1,\mathbf{s}_2)=\frac{\sum_{i=1}^{n}\left(\mathbf{s}_1-\overline{\mathbf{s}}_1\right)\left(\mathbf{s}_2-\overline{\mathbf{s}}_2\right)}{\sqrt{\sum_{i=1}^{n}\left(\mathbf{s}_1-\overline{\mathbf{s}}_1\right)^2}\sqrt{\sum_{i=}^{n}\left(\mathbf{s}_2-\overline{\mathbf{s}}_2\right)^2}} \tag{5}$$

where $\overline{\mathbf{s}}_1$ and $\overline{\mathbf{s}}_2$ are the arithmetic means of their respective SIVV signal vectors. As with the other fidelity measures discussed, the correlation of SIVV signal vectors also shows (via Figure 14) increases with 15:1 compression for some devices with JPEG 2000 compression. However, for some devices this metric shows higher median values with WSQ compression at 0.75 bpp.

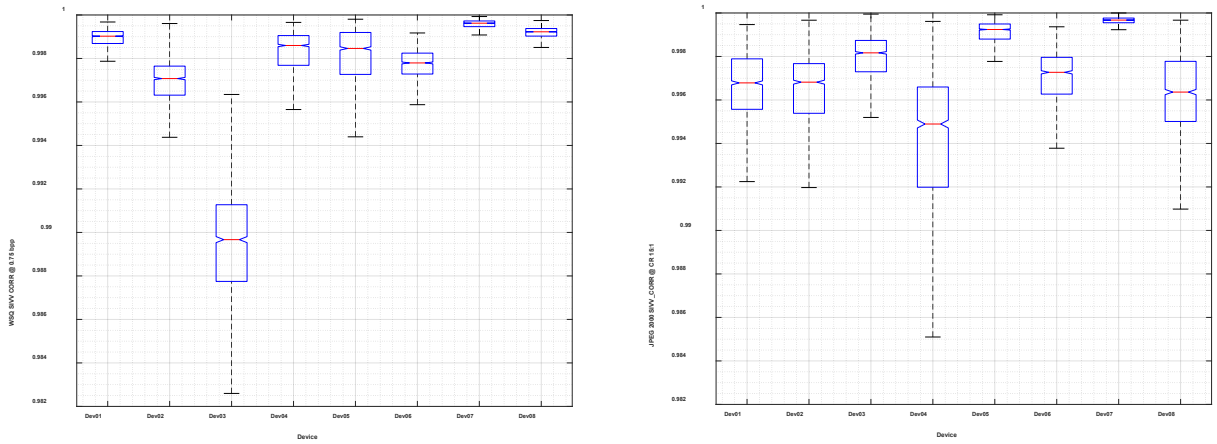


Figure 14 – Distribution of product moment correlation coefficients of SIVV signals for images compressed with a WSQ CODEC at 0.75 bpp (left) and images compressed with a JPEG 2000 CODEC at a target compression ratio of 15:1 (right).

## 4.5. SIVV Difference by Frequency Band

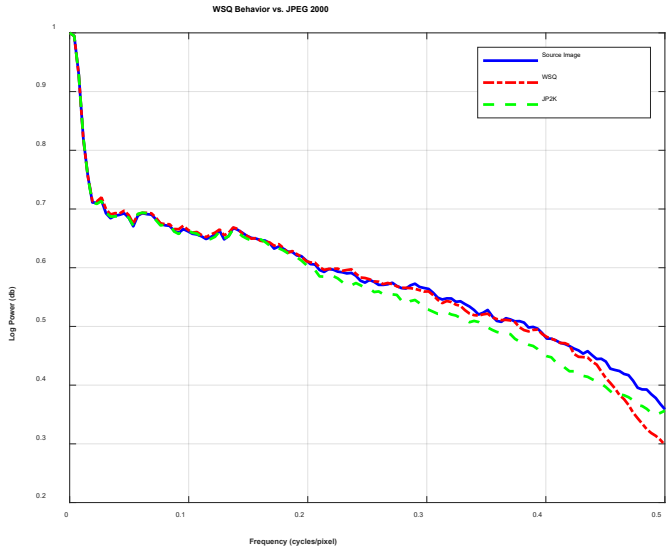


Figure 15 – Comparison of typical SIVV signals for a source original image and those of WSQ and JPEG 2000 (JP2K) compressed versions of the source image. As noted in [14], WSQ retains spectral information through bands three and four whereas the JPEG 2000 spectrum begins to depart from band 2.

As we reported in[15], WSQ and JPEG 2000 differ with respect to preservation of frequency content of images. In Figure 15 we see the SIVV spectra of a source image and of two versions of that image compressed using WSQ and JPEG 2000 CODECs respectively. As is characteristic of lossy image compression, information is discarded in the compression process, generally at frequencies less perceptible by humans or the mechanized system interpreting the imagery. In the present comparison, however, we see important differences in the spectra of the decoded images. WSQ was designed specifically for friction ridge images. Accordingly, its spectrum tracks very closely to that of its non-compressed source, retaining spectral power until the highest frequency band from 0.4 – 0.5 cycles/pixel. By contrast, JPEG 2000, developed as a general-purpose CODEC shows power loss beginning at the start of band 2 (0.2 cycles/pixel) and decreasing steadily through the final high frequency band.

It should be noted that Part 2 of the JPEG 2000 standard provides for proprietary extensions for modifying the wavelet decomposition such that JPEG 2000 might more closely approximate that of WSQ. However, unless the proprietary elements of Part 2 become “royalty free” they are not likely to be widely used among law enforcement organizations for which NIST biometric data compression recommendations are directed, and as such, were not examined.

We partition the difference in the SIVV signals into five partitions of width 0.1 cycle/pixel from 0.0 to 0.5 cycles/pixel as shown in Table 4.

Table 4 – SIVV Partitions

| Band | Interval |
|---|---|
| 1 | [0.0, 0.1] |
| 2 | (0.1, 0.2] |
| 3 | (0.2, 0.3] |
| 4 | (0.3, 0.4] |
| 5 | (0.4, 0.5] |

We calculate the median absolute difference between SIVV signals of source images and corresponding decoded images having been compressed with WSQ and JPEG 2000 CODECs. WSQ is applied with 0.75 bpp specified and JPEG 2000 at the 15:1 compression ratio. The median absolute differences for JPEG 2000 are shown in Figure 16. Here we see that with few exceptions absolute SIVV difference increases from frequency band 2 and continues to increase though band 5.

In Figure 16 we compare absolute SIVV difference with WSQ compression at 0.75 bpp and redisplay this metric for JPEG 2000 compression at 15:1. With WSQ compression the displacement of spectra is generally low up to band 5. The increase in this metric for JPEG 2000 at 15:1 compression ratio is considerably larger than for WSQ.

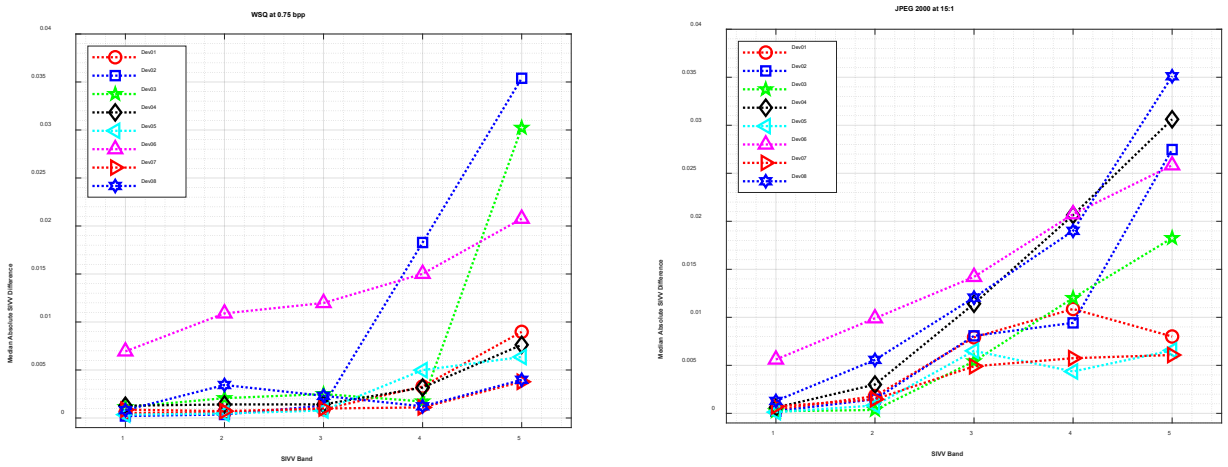


Figure 16 – Median absolute difference of SIVV spectra for compressed and non-compressed source images for WSQ at 0.75 bpp (left) and JPEG 2000 at a 15:1 compression ratio (right). Note the much greater deviation from the non-compressed spectra beginning at band 2 for JPEG 2000.

This loss of spectral power with JPEG 2000 compression may account for why in [14] human examiners were able to detect loss of Level 3 detail at JPEG 2000 compression ratios greater than 10:1 even as other fidelity measures suggest that higher compression levels might be feasible with JPEG 2000. We also suggest that, for most devices, the SIVV Correlation metric described in Section 4.4 shows closer correspondence of power spectra.

## 5. Discussion and Conclusions

Several fidelity metrics applied to compressed contact and contactless fingerprint images suggest that JPEG 2000 as specified in [28], might be preferred over WSQ for some devices. However, a closer look at spectral power shows that as first observed in [15], WSQ tends to preserve power in the middle frequency bands that most likely contain fingerprint features at Levels 2 and 3. This is an effect of the WSQ wavelet decomposition tailored specifically for fingerprints in contrast to that of the more general-purpose JPEG 2000. Despite measured differences in the effects of compression on image fidelity, statistical comparison of match score distributions for the nine compression treatments was unable to detect statistically significant differences among any of the compression treatments applied to fingerprint images collected from both contact and contactless devices, i.e., we failed to reject the null hypothesis that the samples are all drawn from the same distribution. At least for the law enforcement automated fingerprint comparison system used here, compression treatment had no statistically significant impact on match scores when examined either via comparison of distributions or AUC analysis.

Accordingly, the present results find no compelling reason to depart from application of conventional WSQ compression to 500 ppi contactless-collected fingerprint images. We do note that these conclusions apply only to the nominal use case involving automated fingerprint comparison and not to comparison by trained latent fingerprint examiners. Moreover, they are limited further by the small size of the dataset and might later be revised as more contactless data becomes available.

Perhaps the advantages of the WSQ CODEC might derive from its ability to adapt the degree of data loss to the spatial frequency complexity of the image. As we observed previously in Figure 2, the variable compression ratio of WSQ compression results from the algorithm adjusting the level of compression to the spatial frequency content of the image – probably a desirable feature for compression of the texturally complex contactless fingerprints.

## References


[1] Bradley, Jonathan N., Brislawn, Christopher M., Hopper, Thomas. (1993). "FBI wavelet/scalar quantization standard for grayscale fingerprint image compression", SPIE Conference on Visual Information Processing II, eds. Huck, Friedrich O., Juday, Richard D. pp. 293-304.

[2] Bradley, J. N., Brislawn, C. M. (1994). "The wavelet/scalar quantization compression standard for digital fingerprint images". IEEE International Symposium on Circuits and Systems, 1994. ISCAS '94., 1994. Vol 3. pp. 205-208.

[3] Brislawn, Christopher M. (1996). "Wavelet Scalar Quantization Compression Standard for Fingerprint Images". Proceeding Conference on Signal Image Processing and Applications.

[4] Brislawn, Christopher M. (2002). The FBI Fingerprint Image Compression Standard. (Downloaded from https://www.osti.gov/servlets/purl/231283 , 03/24/2022)

[5] FBI Criminal Justice Information Services (CJIS) (1997). WSQ Grayscale Fingerprint Image Compression Specification. IAFIS-IC-0110(V3). December 19, 1997.

[6] Fitzpatrick, M. Et al. 1994, "WSQ Compression / Decompression Algorithm Test Report", IAI Annual Conference.

[7] Hopper, T., Preston, F. (1992). "Compression of grey-scale fingerprint images", Proceedings of Data Compression Conference, 1992. DCC '92. pages 309-318.

[8] Taubman, D. And Marcellin. (2002). JPEG 2000: Image compression fundamentals, standards and practice. Boston, Kluwer Academic Publishers, 795 pages.

[9] Taubman, DS. & Marcellin, MW. (2002). "JPEG 2000: Standard for interactive imaging". Proceedings of the IEEE, vol 90(8), pp. 1336 - 1357.

[10] Ko, K. (2007), User's Guide to NIST Biometric Image Software (NBIS), NIST Interagency/Internal Report (NISTIR), National Institute of Standards and Technology, Gaithersburg, MD, [online], https://doi.org/10.6028/NIST.IR.7392 (Accessed March 28, 2023)

[11] Ko, K. and Salamon, W. NIST Biometric Image Software (NBIS), Release 5.0.0, National Institute of Standards and Technology, https://www.nist.gov/itl/iad/image-group/products-and-services/image-group-open-source-server-nigos#Releases.

[12] Chai, D., Bouzerdoum, A. (2001). "JPEG 2000 image compression: an overview". Proceedings of The Seventh Australian and New Zealand 2001 Intelligent Information Systems Conference, pp. 237-241.

[13] OpenJPEG library : an open-source JPEG 2000 CODEC written in C. http://www.openjpeg.org/ (Retrieved 03/31/2022).

[14] Orandi, S., Libert, J.M., Grantham, J.D., Ko., K., Wood, S. S., Byers, F., Bandini, B., and Harvey, S.G., Compression Guidance for 1000 ppi Friction Ridge Imagery, NIST Special Publication 500-289, National Institutes of Standards and Technology, Gaithersburg, MD., February 2014. http://nvlpubs.nist.gov/nistpubs/specialpublications/NIST.SP.500-289.pdf Retrieved 07/31/2017.

[15] Libert, J.M., Orandi, S., Grantham, J. D. "Comparison of the WSQ and JPEG 2000 Image Compression Algorithms On 500 ppi Fingerprint Imagery", NISTIR 7781, April 24, 2012. https://tsapps.nist.gov/publication/get_pdf.cfm?pub_id=910658 , 03/24.2022)

[16] Libert, J.M., Grantham, J.; Orandi, S. "A 1D Spectral Image Validation/Verification Metric for Fingerprints". NISTIR 7599, August 19, 2009.

[17] Libert, J., Grantham, J., and Watson, C. Compression Guidance for 1000 ppi Palm and Hand Friction Ridge Imagery, NIST Interagency Report (NISTIR) 8260, July 2019. https://nvlpubs.nist.gov/nistpubs/ir/2019/NIST.IR.8260.pdf
[18] Galton, F. (2005). Fingerprints. Mineola, NY: Dover Publications. (Original work published 1892)
[19] Jain, A., "Pores and Ridges: High-Resolution Fingerprint Matching Using Level 3 Features", IEEE Transactions on Pattern Analysis and Machine Intelligence, Vol. 29, No. 1, January 2007.
[20] Girod, Bernd (1993). "What's wrong with mean-squared error?" Digital images and human vision, Andrew B. Watson, ed. MIT Press, pages 207-220.
[21] Huynh-Thu, Q., Ghanbari, M. (2008). "Scope of validity of PSNR in image/video quality assessment". Electronics Letters, Vol. 4, No. 13, pp. 800-801.
[22] Wang, Z. and A. C. Bovik, "Mean squared error: love it or leave it?", IEEE Signal Processing Magazine, vol. 26, pp.98-117, 2009
[23] Horé, A. and Ziou, D. "Image Quality Metrics: PSNR vs. SSIM," 2010 20th International Conference on Pattern Recognition, 2010, pp. 2366-2369, doi: 10.1109/ICPR.2010.579.
[24] Wang, Z., A. C. Bovik, H. R. Sheikh, and E. P. Simoncelli. "Image Quality Assessment: From Error Visibility to Structural Similarity." IEEE Transactions on Image Processing. Vol. 13, Issue 4, April 2004, pp. 600–612.
[25] Sheikh, H. R. and A. C. Bovik, "Image information and visual quality", IEEE Transactions on Image Processing, vol. 15, no. 2, pp. 430-444, 2006.
[26] Libert, J. , Grantham, J. , Bandini, B. , Ko, K. , Orandi, S. and Watson, C. (2020), Interoperability Assessment 2019: Contactless-to-Contact Fingerprint Capture, NIST Interagency/Internal Report (NISTIR), National Institute of Standards and Technology, Gaithersburg, MD, [online], https://doi.org/10.6028/NIST.IR.8307 (Accessed June 7, 2022)
[27] Orandi, S. , Libert, J. , Bandini, B. , Ko, K. , Grantham, J. and Watson, C. (2020), Evaluating the Operational Impact of Contactless Fingerprint Imagery on Matcher Performance, NIST Interagency/Internal Report (NISTIR), National Institute of Standards and Technology, Gaithersburg, MD, [online], https://doi.org/10.6028/NIST.IR.8315 (Accessed June 7, 2022).
[28] Special Publication (NIST SP) - 500-290e3: "American National Standard for Information Systems — Data Format for the Interchange of Fingerprint, Facial & Other Biometric Information, ANSI/NIST-ITL 1-2011 NIST Special Publication 500-290 Edition 3. August 22, 2016. http://nvlpubs.nist.gov/nistpubs/SpecialPublications/NIST.SP.500-290e3.pdf
[29] Libert, J., Grantham, J., Bandini, B., Ko, K., Orandi, S., Watson, C., "Interoperability Assessment 2019: contactless-to-Contact Fingerprint Capture", NISTIR 8307, National Institute of Standards and Technology, Gaithersburg, MD. https://doi.org/10.6028/NIST.IR.8307.
[30] The MathWorks, Inc. (2022). *MATLAB version: 9.13.0 (R2022b)*. Accessed: January 01, 2023. Available: https://www.mathworks.com
[31] Qin, G, Hotilovac, L (2008). Comparison of non-parametric confidence intervals for the area under the ROC curve of a continuous-scale diagnostic test. Stat Meth Med Res, 17:207-21.
[32] *Kruskal*, W.H. and *Wallis*, W.A. Use of Ranks in One-Criterion Variance Analysis. Journal of the American Statistical Association, 47, 583-621, 1952.

[33] Orandi, S., Libert, J., Bandini, Ko, K., J., Grantham, B., Watson, C., "Evaluating the Operational Impact of Contactless Fingerprint Imagery on Matcher Performance", NISTIR 8315, National Institute of Standards and Technology, Gaithersburg, MD. https://doi.org/10.6028/NIST.IR.8315.
[34] Orandi, S., Libert, J. M., Grantham, J. D., Ko, K., Wood, S.S., Wu, J. Effects of JPEG 2000 Image Compression on 1000 ppi Fingerprint Imagery, NIST Interagency Report 7778, National Institutes of Standards and Technology, Gaithersburg, MD. Retrieved 01/10/2023.
[35] Orandi, S., Libert, J.M., Grantham, Petersen, L. P., "Effects of JPEG 2000 Lossy Image Compression on 1000 ppi Latent Fingerprint Imagery", NIST Interagency Report 7780, National Institutes of Standards and Technology, Gaithersburg, MD. http://www.nist.gov/customcf/get_pdf.cfm?pub_id=914513.
[36] Libert, J. M., Orandi, S., and Grantham, J. D., "Comparison of the WSQ and JPEG 2000 Image Compression Algorithms On 500 ppi Fingerprint Imagery", NIST Interagency Report 7781, National Institute of Standards and Technology, Gaithersburg, MD. http://www.nist.gov/customcf/get_pdf.cfm?pub_id=910658
[37] Libert, J. M., Orandi, S., Grantham, J.D., "Effects of Decomposition Levels and Quality Layers with JPEG 2000 Compression of 1000 ppi Fingerprint Images", NIST Interagency Report 7939, National Institutes of Standards and Technology, Gaithersburg, MD. http://nvlpubs.nist.gov/nistpubs/ir/2013/NIST.IR.7939.pdf.
[38] Galton, F. (2005). Fingerprints. Mineola, NY: Dover Publications. (Original work published 1892)
[39] Jain, A., "Pores and Ridges: High-Resolution Fingerprint Matching Using Level 3 Features", IEEE Transactions on Pattern Analysis and Machine Intelligence, Vol. 29, No. 1, January 2007.

## Appendix A. Box and Whisker Plots

In the metric analyses above we summarize the measurement results in most cases using the data visualization graphic known as the boxplot or box and whisker plot. This method enables simultaneous display of measurement distributions for multiple experimental conditions, or in the present case, devices or comparisons of measurements between devices.

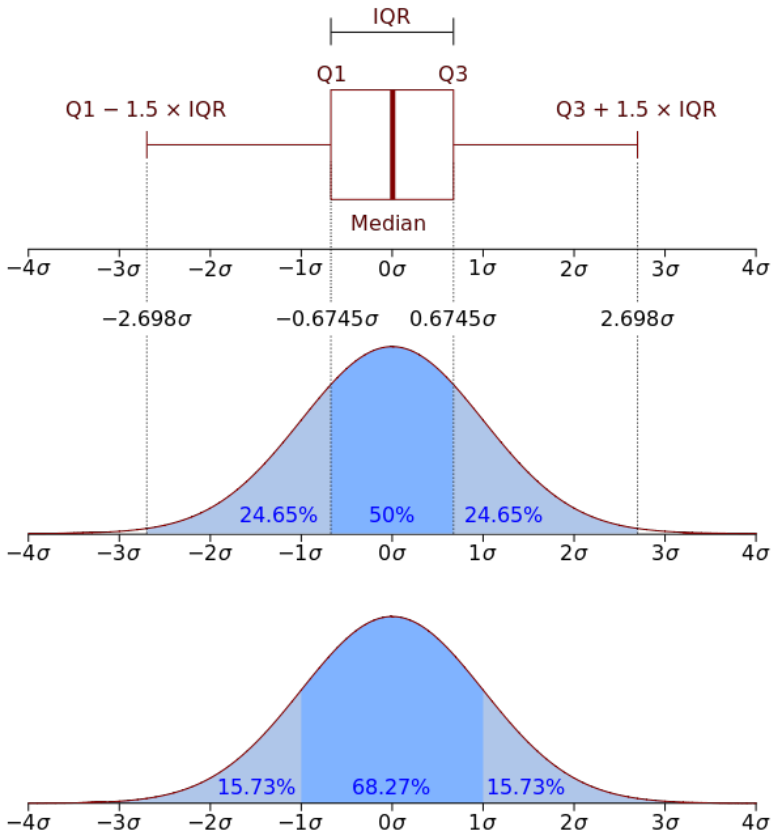


Figure 17 – Relationship between the boxplot of normally distributed data compared to the standard normal distribution for illustrative purposes. (Graphic from [WMC])

In the plots above, we see that the outstanding feature of the boxplot is, of course, the box having the median marked by the central line. In the boxplots used in the present study, the median is surrounded by a notch representing the 95 % confidence interval about the median value. Interpreting the boxplot, it is significant that the box contains 50 % of the distribution and 24.65 % between the limits of the box, Q1 and Q3, and the ends of each whisker. Note that corresponding to the normal distribution, this leaves approximately 0.35 % of the distribution beyond the limits of the whiskers. In these boxplots, these values, considered outliers, are omitted from the display.

## Appendix B. List of Symbols, Abbreviations, and Acronyms

The abbreviations and acronyms of Table 1 are used in many parts of this document.

Table 5 – Abbreviations and Terms

| | |
|---|---|
| ANSI/NIST-ITL | NIST Special Publication 500-290e3 ANSI/NIST-ITL 1-2011 Update:2015 American National Standard for Information Systems - Data Format for the Interchange of Fingerprint, Facial & Other Biometric Information |
| bpp | Bits per pixel |
| CODEC | Coder/decoder (or compression/decompression algorithm, module, software) |
| CR | Compression Ratio |
| FBI | Federal Bureau of Investigation |
| FTIR | Frustrated Total Internal Reflection – the optical phenomenon used by some fingerprint sensing devices for image formation |
| gallery | Biometric reference database or biometric enrolment database |
| JPEG | Joint Photographic Experts Group – ISO/IEC committee developing standards for image compression – also used as the name of the CODEC developed in accordance with the standard specified by this body. |
| LEO | Law Enforcement Organization |
| NIST | National Institute of Standards and Technology |
| NISTIR | NIST Interagency Report |
| PNG | Portable Network Graphic – a lossless image format |
| ppi | Pixels per inch |
| ppmm | Pixels per millimeter |
| probe | A biometric sample compared to the biometric reference database (gallery) |
| PSNR | Peak Signal-To-Noise Ratio |
| SIVV | Spectral Image Validation/Verification metric |
| SSIM | Structural Similarity Index Metric (Measure) |
| WSQ | The Wavelet Scalar Quantization algorithm for compression of fingerprint imagery |